Tchernev G, Ananiev J, Cardoso JC, Wollina U, Verma SB, Patterson JW, Dourmishev LA, Tronnier M, Okamoto H, Mizuno K, Kanazawa N, Gulubova M, Manolova I, Salaro C	Sarcoidosis and molecular mimicry-important etiopathogenetic aspects: current state and future directions	Wien Klin Wochenschr	124	227-238	2012
Ikeda T, Kanazawa N, Furukawa F	Hydroxychloroquine administration for Japanese lupus erythematosus in Wakayama: A pilot study	J Dermatol	39	531-535	2012
Kuwahara J, Li HJ, Kanazawa N, Furukawa F	Attempts to induce auricular hematoma in a mouse model of collagen-induced arthritis	Aesthet Dermatol	22	118-123	2012
Wada T, Toga A, Sakakibara Y, Toma T, Shigemura T, Agematsu K, Yachie A	Clonal expansion of Epstein-Barr virus (EBV)-infected γδ T cells in patients with chronic active EBV disease and hydroa vacciniforme-like eruptions.	Int J Hematol	96(4)	443-9	2012
Wada T, Muraoka M, Toma T, Imai T, Shigemura T, Agematsu K, Haraguchi K, Moriuchi H, Oh-Ishi T, Kitoh T, Ohara O, Morio T, Yachie A	Rapid Detection of Intracellular p47phox and p67phox by Flow Cytometry; Useful Screening Tests for Chronic Granulomatous Disease.	J Clin Immunol		in press	
Shimizu M, Yachie A	Compensated inflammation in systemic juvenile idiopathic arthritis: role of alternatively activated macrophages.	Cytokine	60	226-232	2012
Shimizu M, Nakagishi Y, Kasai K, Yamasaki Y, Miyoshi M, Takei S, Yachie A	Tocilizumab masks the clinical symptoms of systemic juvenile idiopathic arthritis-associated macrophage activation syndrome: the diagnostic significance of interleukin-18 and interleukin-6.	Cytokine	58(2)	287-294	2012
Iwata K, Toma T, Yachie A	38-year-old woman with recurrent abdominal pain, but no fever.	Int J Gen Med	5	265-268	2012

Isoda T, Mitsuiki N, Ohkawa T, Kaneko S, Endo A, Ono T, Aoki Y, Tomizawa D, Kajiwara M, Araki S, Nagasawa M, Morio T, Takagi M, Mizutani S	Irreversible Leukoencephalopathy After Reduced-intensity Stem Cell Transplantation in a Dyskeratosis Congenita Patient With TINF2 Mutation.	J Pediatr Hematol Oncol		in press	
Kamae C, Nakagawa N, Sato H, Honma K, Mitsuiki N, Ohara O, Kanegane H, Pasic S, Pan-Hammerstrom Q, van Zelm M.C., Morio T, Imai K, Nonoyama S	Classification of common variable immunodeficiency by quantification of T cell receptor and Ig kappa-deleting recombination excision circles.	J Allerg Clin Immunol		in press	
Kawasaki Y, Toyoda H, Otsuki S, Iwasa T, Iwamoto S, Azuma E, Itoh-Habe N, Wada H, Fujimura Y, Morio T, Imai K, Mitsuiki N, Ohara O, Komada Y	A novel Wiskott-Aldrich syndrome protein mutation in an infant with thrombotic thrombocytopenic purpura.	Eur J Haematol	90	164-168	2012
Shimizu M, Kanegane H, Wada T, Motoyoshi Y, Morio T, Candotti F, Yachie A	Aberrant glycosylation of IgA in Wiskott-Aldrich syndrome and X-linked thrombocytopenia.	J Allergy Clin Immunol.	131(2)	587-590.e3	2013
Yoshimi A, Kamachi Y, Imai K, Watanabe N, Nakadate H, Kanazawa T, Ozono S, Kobayashi R, Yoshida M, Kobayashi C, Hama A, Muramatsu H, Sasahara Y, Jakob M, Morio T, Ehl S, Manabe A, Niemeyer C, Kojima S	Wiskott-Aldrich syndrome presenting with a clinical picture mimicking juvenile myelomonocytic leukaemia.	Pediatr Blood Cancer		in press	
Isoda T, Takagi M, Piao J, Nishii R, Masaki S, Masuda K, Ikawa T, Azuma M, Morio T, Kawamoto H, Mizutani S	Process for immune defect and chromosomal translocation during early thymocyte development lacking ATM.	Blood	120	789-799	2012
Honda F, Kano H, Kanegane H, Nonoyama S, Kim E-S, Lee S-K, Takagi M, Mizutani S, Morio T	Btk negatively regulates ROS production and stimulation-induced apoptosis in human neutrophils.	Nature Immunol	13	369-378	2012

Kuramitsu M, Sato-Otsubo A, Morio T, Takagi M, Toki T, Terui K, RuNan W, Kanno H, Ohga S, Ohara A, Kojima S, Kitoh T, Goi K, Kudo K, Matsubayashi T, Mizue N, Ozeki M, Masumi A, Momose H, Takizawa K, Mizukami T, Yamaguchi K, Ogawa S, Ito E	Extensive gene deletions in Japanese patients with Diamond-Blackfan anemia.	Blood	119	2376-2384	2012
Sato R, Iizumi S, Kim E-S, Honda F, Lee S-K, Adachi N, Koyama H, Mizutani S, Morio T	Impaired cell adhesion, apoptosis, and signaling in WASP-gene disrupted Nalm-6 pre-B cells and recovery of cell adhesion using a transducible form of WASp.	Int J Hematol	95	299-310	2012
Ma CS, Avery DT, Chan A, Batten M, Bustamante J, Boisson-Dupuis S, Arkwright PD, Minegishi Y, Nonoyama S, French MA, Choo S, Peake J, Wong M, Cook MC, Fulcher DA, Casanova JL, Deenick EK, Tangye SG	Functional STAT3 deficiency compromises the generation of human T follicular helper cells.	Blood	26;119	3997-4008	2012
Ishida H, Imai K, Homma K, Tamura S, Imamura T, Itoh M, Nonoyama S	GATA-2 anomaly and clinical phenotype of a sporadic case of lymphedema, dendritic cell, monocyte, B- and NK-cell (DCML) deficiency, and myelodysplasia.	Eur J Pediatr	171	1273-1276	2012
Suri D, Singh S, Rawat A, Gupta A, Kamae C, Honma K, Nakagawa N, Imai K, Nonoyama S, Oshima K, Mitsuiki N, Ohara O, Bilhou-Nabera C, Proust A, Ahluwalia J, Dogra S, Saikia B, Walker Minz R, Sehgal S	Clinical profile and genetic basis of Wiskott-Aldrich syndrome at Chandigarh, north India.	Asian Pac J Allergy Immunol	30	71-78	2012

Nakaoka H, Kanegane H, Taneichi H, Miya K, Yang X, Nomura K, Takezaki S, Yamada M, Ohara O, Kamae C, Imai K, Nonoyama S, Wada T, Yachie A, Hershfield MS, Ariga T, Miyawaki T	Delayed onset adenosine deaminase deficiency associated with acute disseminated encephalomyelitis.	Int J Hematol	95	692-696	2012
Yang X, Kanegane H, Nishida N, Imamura T, Hamamoto K, Miyashita R, Imai K, Nonoyama S, Sanayama K, Yamaide A, Kato F, Nagai K, Ishii E, Zelm M, Latour S, Zhao X, Miyawaki T	Clinical and genetic characteristics of XIAP deficiency in Japan.	J Clin Immunol	32	411-420	2012
Kakiuchi S, Nonoyama S, Wakamatsu H, Kogawa K, Wang L, Kinoshita-Yamaguchi H, Takayama-Ito M, Lim CK, Inoue N, Mizuguchi M, Igarashi T, Saijo M	Neonatal herpes encephalitis caused by a virologically confirmed acyclovir resistant herpes simplex virus type 1.	J Clin Microbiol	51	356-359	2013
Shirasaki Y, Yamagishi M, Shimura N, Hijikata A, Ohara O	Toward an understanding of immune cell sociology: real-time monitoring of cytokine secretion at the single-cell level.	IUBMB Life	65(1)	28-34	2013
Oshima K, Nagase T, Imai K, Nonoyama S, Obara M, Mizukami T, Nunoi H, Kanegane H, Kuribayashi F, Amemiya S, Ohara O	A Dual Reporter Splicing Assay Using HaloTag-containing Proteins.	Curr Chem Genomics	6	27-37	2012
Takezaki S, Yamada M, Kato M, Park MJ, Maruyama K, Yamazaki Y, Chida N, Ohara O, Kobayashi I, Ariga T	Chronic mucocutaneous candidiasis caused by a gain-of-function mutation in the STAT1 DNA-binding domain.	J Immunol.	189(3)	1521-1526	2012

Mohammadzadeh I, Yeganeh M, Aghamohammadi A, Parvaneh N, Behniafard N, Abolhassani H, Tabassomi F, Hemmat M, Kanegane H, Miyawaki T, Ohara O, Rezaei N	Severe primary antibody deficiency due to a novel mutation of mu heavy chain.	J Investig Allergol Clin Immunol	22(1)	78-79	2012
Nakaoka H, Kanegane H, Taneichi H, Miya K, Yang X, Nomura K, Takezaki S, Yamada M, Ohara O, Kamae C, Imai K, Nonoyama S, Wada T, Yachie A, Hershfield MS, Ariga T, Miyawaki T	Delayed onset adenosine deaminase deficiency associated with acute disseminated encephalomyelitis.	Int J Hematol	95(6)	692-696	2012
横田俊平、西小森隆太 高田英俊、菊地雅子 野澤智、金高太一 木澤敏毅、宮前多佳子 森雅亮、平家俊男 原寿郎、今川智之	クリオピリン関連周期性発熱症候群に対する生物学的製剤治療の手引き(2012)　カナキヌマブ(総説)	日本小児科学会雑誌	116巻9号	1337-1341	2012
西小森隆太、井澤和司 平家俊男	【クローズアップ感染症】 PFAPA以外の周期性発熱症候群についての知見(解説/特集)	小児内科	44巻7号	1221-1226	2012
西小森隆太、井澤和司 平家俊男	原発性免疫不全症における臨床遺伝学 日本における自己炎症疾患の遺伝子診断について(解説)	日本遺伝カウンセリング学会誌	33巻1号	63-68	2012
西小森隆太、平家俊男	自己炎症症候群	小児内科	44巻増刊号	290-291	2012
斎藤潤、中畑龍俊	疾患特異的iPS細胞	再生医療	Vol.12 No.1	19-32	2013
原　寿郎	原発性免疫不全症(PID)－悪性腫瘍，血液疾患を合併するPIDを中心に－	日本小児血液・がん学会雑誌	49(3)	237-241	2012
高田英俊、大賀正一 原　寿郎	自己炎症症候群.　特集　知っておきたい最新の免疫不全症候群分類－診断から治療まで－	小児科診療	76 (3)	印刷中	2012
大西秀典、寺本貴英 久保田一生、近藤直実	皮膚症状からみた自己炎症性症候群	小児科	53	1201-1209	2012
井田弘明、有馬和彦 金澤伸雄、吉浦孝一郎	中條-西村症候群の原因遺伝子とプロテアソーム機能異常	リウマチ科	47(6)	654-660	2012
井田弘明、福田孝昭	自己炎症症候群の定義と分類	九州リウマチ	32(2)	75-78	2012
井田弘明、福田孝昭	自己炎症症候群	日本臨床	70(suppl 8)	561-568	2012
井田弘明	自己炎症症候群	日本医事新報	4615	78-83	2012

井田弘明、有馬和彦 金澤伸雄、吉浦孝一郎	プロテアソーム病	炎症と免疫	20(6)	609-614	2012
有馬和彦、井田弘明 金澤伸雄、吉浦孝一郎	プロテアソームの機能阻害型遺伝子変異が新規自己炎症疾患である中條-西村症候群を引き起こす	細胞工学	31	68-69	2012
神戸直智、中村悠美	連載「自己炎症症候群の多様性」　CAPSでみられるヒスタミン非依存性蕁麻疹	炎症と免疫	20	183-188	2012
神戸直智	特集「蕁麻疹患者のQOL向上術」蕁麻疹様皮疹を呈するクリオピリン関連周期性症候群の診断と管理.	Monthly Book Derma デルマ	194	63-69	2012
神戸直智、中村悠美	特集「アナフィラキシーショック」NLRP3インフラマソームを介したマスト細胞の活性化	臨床免疫・アレルギー科	58	560-564	2012
神戸直智	自己炎症症候群と皮膚疾患の関連　ー治りにくい蕁麻疹（それと乾癬）についてー	日皮会誌	122	3286-3288	2012
金澤伸雄	NOD2関連疾患	炎症と免疫	20	517-522	2012
金澤伸雄	皮膚-紅斑など皮膚症状から診断へ	小児内科	44	85-89	2012
上松一永	【小児疾患の診断治療基準(第4版)】 (第2部)疾患　生体防御・免疫不全　重症複合免疫不全症	小児内科	44(11)	224-225	2012
森尾友宏	先天性免疫不全症の病態と思春期以降のマネジメント	血液内科	65	599-607	2012
森尾友宏	【クローズアップ感染症】〈感染性疾患の基礎的な知見の進歩・概念の変化>感染症と自然免疫	小児内科	44	959-965	2012
森尾友宏	【サイトカインのすべて(完全改訂版)】 サイトカイン投与およびサイトカイン抑制による治療 免疫不全症	臨床免疫・アレルギー科	57	838-844	2012
森尾友宏	原発性免疫不全症における臨床遺伝学 T細胞系免疫異常症における遺伝子診療	日本遺伝カウンセリング	33	49-53	2012
森尾友宏	分類不能型免疫不全症	日本臨牀	70	2011-2021	2012
森尾友宏	分類不能型免疫不全症 Update	日本臨床免疫	35	14-22	2012

Mod Rheumatol
DOI 10.1007/s10165-012-0769-8

REVIEW ARTICLE

Guidance on the use of canakinumab in patients with cryopyrin-associated periodic syndrome in Japan

Shumpei Yokota · Ryuta Nishikomori · Hidetoshi Takada · Masako Kikuchi · Tomo Nozawa · Taichi Kanetaka · Toshitaka Kizawa · Takako Miyamae · Masaaki Mori · Toshio Heike · Toshiro Hara · Tomoyuki Imagawa

Received: 18 June 2012 / Accepted: 5 September 2012

Abstract Cryopyrin-associated periodic syndrome (CAPS) is an orphan disease with incidence of about one in 1,000,000 persons. This autoinflammatory disease develops in the neonatal period or early childhood, with various inflammatory symptoms occurring repeatedly throughout the patient's lifetime. It is caused by abnormality of the NLRP3 protein which mediates the intracellular signal transduction mechanism of inflammatory processes, resulting in continuous overproduction of interleukin (IL)-1β, which induces chronic inflammation and progressive tissue damage. Definitive diagnosis of CAPS is difficult, and treatment has also been difficult because of a lack of effective medications in Japan. Clinical studies of human anti-human IL-1β monoclonal antibody (canakinumab) treatment were conducted in Japan, and approval was granted for therapeutic use of canakinumab for CAPS in September 2011. Similar to other biological drugs, canakinumab is clinically highly effective. However, sufficient attention to the method of use and adverse drug reactions is necessary. This guidance describes the use of canakinumab in Japan for CAPS in relation to exclusion criteria, method of use, evaluation criteria, and adverse drug reactions.

Keywords Canakinumab · Cryopyrin-associated periodic syndrome · Human anti-human IL-1β monoclonal antibody · Interleukin-1β

S. Yokota (✉) · M. Kikuchi · T. Nozawa · T. Kanetaka · T. Kizawa · T. Miyamae · M. Mori · T. Imagawa
Department of Pediatrics, Yokohama City University School of Medicine, 3-9, Fukuura, Kanazawa-ku, Yokohama 236-0004, Japan
e-mail: syokota@med.yokohama-cu.ac.jp

R. Nishikomori · T. Heike
Department of Pediatrics, Graduate School of Medicine, Kyoto University, Kyoto, Japan

H. Takada · T. Hara
Department of Pediatrics, Graduate School of Medical Sciences, Kyushu University, Fukuoka, Japan

Introduction

Cryopyrin-associated periodic syndrome (CAPS) is an autoinflammatory disease that develops in the neonatal period or early childhood, with various inflammatory symptoms. Patients experience recurrent rash, articular symptoms, fever, and headache associated with chronic meningitis, as well as progressive visual and auditory impairment. Many patients have poor prognosis, and a large proportion develop amyloidosis.

CAPS is classified into the following three types according to its symptoms: familial cold autoinflammatory syndrome (FCAS), Muckle–Wells syndrome (MWS), and neonatal-onset multisystem inflammatory disease (NOMID). All types are associated with overproduction of interleukin (IL)-1β, which induces inflammation [1, 2] and chronic tissue damage. The overproduction is caused by a mutation of the *NLRP3* gene [3–6], which mediates responses to infectious agents, tissue damage, and intracellular proteins derived from apoptosis.

The incidence of CAPS is about one in 1,000,000 persons. Definitive diagnosis of CAPS is difficult, and treatment has also been difficult because of a lack of effective medications in Japan. Therefore, clinical studies of human anti-human IL-1β monoclonal antibody (canakinumab) treatment were conducted in Japan, and approval was granted for therapeutic use of canakinumab for CAPS in

Published online: 20 October 2012

September 2011. However, canakinumab can also suppress physiological inflammation by neutralizing the activity of IL-1β. Although canakinumab is clinically highly effective, adverse drug reactions will be carefully monitored.

This guidance describes the use of canakinumab for treatment of CAPS in Japan in relation to exclusion criteria, method of use, evaluation criteria, and adverse drug reactions.

Overview of canakinumab

Canakinumab (Ilaris®; Novartis Pharma K.K.) is a recombinant human immunoglobulin G1 monoclonal antibody against human IL-1β expressed in mouse hybridoma SP2/0-Ag14 cells. It neutralizes the activity of IL-1β by binding to IL-1β and inhibiting binding of IL-1β to its receptor [7]. Clinical studies conducted in Japan and other countries have demonstrated that canakinumab promptly improves various inflammation-related symptoms and abnormal laboratory values in CAPS patients by inhibiting the action of IL-1β [8, 9], and that these effects persist for long time [10].

Canakinumab was approved for treatment of CAPS in the USA and Europe in 2009, and had been approved in at least 50 countries as of August 2011. In Japan, the phase I clinical study in healthy volunteers began in December 2006, and the phase III clinical study in CAPS patients began in October 2009. Canakinumab was designated as an orphan drug in August 2010. Based on the results of the Japanese phase I and phase III clinical studies and overseas clinical studies, canakinumab was approved for treatment of CAPS in September 2011.

Guideline for canakinumab treatment of CAPS patients

Indications and use

Canakinumab is indicated for treatment of CAPS. CAPS is classified according to its severity into three types: FCAS [11], MWS [12], and NOMID [13]. Patients with FCAS, which is considered to be a mild form, experience urticarial rash, fever, conjunctivitis, and other symptoms due to cold stimuli. MWS and NOMID are classified according to differences in the timing of onset and severity of symptoms, but there are no other specific differences between these types. Symptoms include fever, urticarial rash, headache, central nervous system inflammation, arthritis, and amyloidosis, depending on the severity. Inflammatory indices such as C-reactive protein (CRP) and serum amyloid A (SAA) are elevated. If these common findings and the following characteristic findings are observed, CAPS should be suspected, specialists who have experience in the prescription of canakinumab should be consulted, and *NLRP3* genetic testing should be performed.

The age of onset of FCAS [11] is just after birth or in early infancy in about 95 % of cases. Inflammatory episodes including rash, fever, and arthralgia occur repeatedly following cold exposure. Inflammatory reactions may last less than 24 h. Conjunctivitis occurs during inflammatory episodes, but hearing loss, periorbital edema, lymphadenopathy, and serositis are not observed. Concomitant amyloidosis is rare. The *NLRP3* gene is mutated in most patients.

The age of onset of MWS [12] is usually during infancy, but some patients develop the disease in childhood or adolescence. Abnormality of the *NLRP3* gene is detected in 65–75 % of cases. Inflammatory symptoms occur repeatedly due to stress, and persist for almost 3 days. Patients experience fever, rash, arthritis, myalgia, headache, conjunctivitis, and uveitis. Sensorineural hearing loss or hearing impairment occurs in 50–70 % of patients, and renal failure due to amyloidosis occurs in about 25 %.

Inflammatory symptoms occur continuously and repeatedly from soon after birth in NOMID [13]. About half of patients have low birth weight. Patients experience fever, urticarial rash, arthritis, headache, conjunctivitis, and episcleritis almost every day. Headache associated with chronic aseptic meningitis, vomiting, and irritability can also occur. Hydrocephalus, sensorineural hearing loss, psychomotor retardation, growth disorders, joint disorders, and amyloidosis develop in the long term. Joint disorders during the developmental stage lead to gait disturbance. About 20 % of patients have poor prognosis before the age of 20 years, and many patients experience progression to amyloidosis.

Contraindications and careful administration of canakinumab are presented in Table 1. There have been no cases of discontinuation of canakinumab to date.

Predose testing

Patients should be carefully screened for common infections, especially otitis media, sinusitis, and respiratory tract infections (including bronchiectasis). Patients must also be screened for tuberculosis with an interview and the following tests: chest X-ray, tuberculin reaction, chest computed tomography (CT), and QuantiFERON® (QFT). As chest X-ray and tuberculin reaction do not always give a definitive diagnosis, chest CT and/or QFT should be performed as necessary. Chest CT is necessary for all pediatric patients. Patients with history of tuberculosis or a suspected tuberculosis infection should be evaluated by physicians with experience in the treatment of tuberculosis, including pulmonologists and radiologists.

Table 1 Contraindications and careful administration of canakinumab

Contraindications	Careful administration
Patients with serious infection (Infection may worsen)	Patients with infection or suspected infection (Infection may worsen)
Patients with active tuberculosis (Symptoms may worsen)	Patients with history of tuberculosis or suspected tuberculosis infection (Tuberculosis may be activated)
Patients with history of hypersensitivity to any of the ingredients of canakinumab	Patients with history of recurring infection (Infection may recur)
	Immunocompromised patients (Infection may be induced)

Canakinumab should only be given after the administration of an antituberculous drug in patients who meet any of the followings criteria:

- Patients with shadows consistent with or indicative of old tuberculosis on chest imaging
- Patients with history of treatment for tuberculosis (including extrapulmonary tuberculosis)
- Patients strongly suspected of having tuberculosis infection in a tuberculin test or interferon gamma response test (QFT)
- Patients with history of close contact with a tuberculosis patient

Dosage and administration (Fig. 1)

Canakinumab is usually administered at 2 mg/kg for CAPS patients with body weight $\leq$40 kg or 150 mg for body weight >40 kg, every 8 weeks as a single dose via subcutaneous injection.

If satisfactory clinical response (resolution of rash and other generalized inflammatory symptoms) has not been achieved, the dose should be gradually increased as appropriate. Maximum dose is 8 mg/kg for body weight $\leq$40 kg or 600 mg for body weight >40 kg [10].

If the patient experiences relapse within 8 weeks after an administration with the maximum dose, an increase of dosing frequency of up to every 4 weeks can be considered.

The dose may be adjusted according to the condition.

Treatment evaluation

Remission criteria (clinical and serological remission) and relapse criteria (clinical and serological relapse) were used in the Japanese clinical studies to evaluate the therapeutic effects of canakinumab in patients with CAPS (Table 2). Clinical remission and relapse were evaluated using the following five levels of symptoms: absent, minimal, mild, moderate, and severe. These five levels of evaluations should be evaluated based on physician's assessment because there are no criteria for each level.

Evaluations of adverse reactions

In clinical studies in Japan, adverse drug reactions occurred in 12 of 19 subjects (63.2 %). Common adverse reactions were nasopharyngitis in three subjects (15.8 %) and stomatitis in two subjects (10.5 %). In clinical studies in other countries, adverse drug reactions occurred in 68 of 169 subjects (40.2 %). Common adverse reactions were headache in seven subjects (4.1 %), weight gain in seven subjects (4.1 %), vertigo in six subjects (3.6 %), and bronchitis in five subjects (3.0 %).

Canakinumab may affect the inflammatory and immunological reactions to viruses, bacteria, and *Mycobacterium tuberculosis* by inhibiting the action of IL-1β, which may lead to worsening of infection. In clinical studies conducted in Japan and other countries, infections including upper respiratory tract infection were reported frequently, and some of these infections were serious. Patients should therefore be carefully monitored for the occurrence, recurrence, and exacerbation of infection during canakinumab therapy.

Immunization during canakinumab therapy

Inactivated vaccines may be administered during canakinumab therapy. Live vaccines should not be given, because a risk of developing infection cannot be ruled out. It is desirable to administer necessary vaccines prior to canakinumab therapy.

Caution

Canakinumab must be used with strict adherence to the indications and contraindications. It is recommended that canakinumab be used by physicians with appropriate

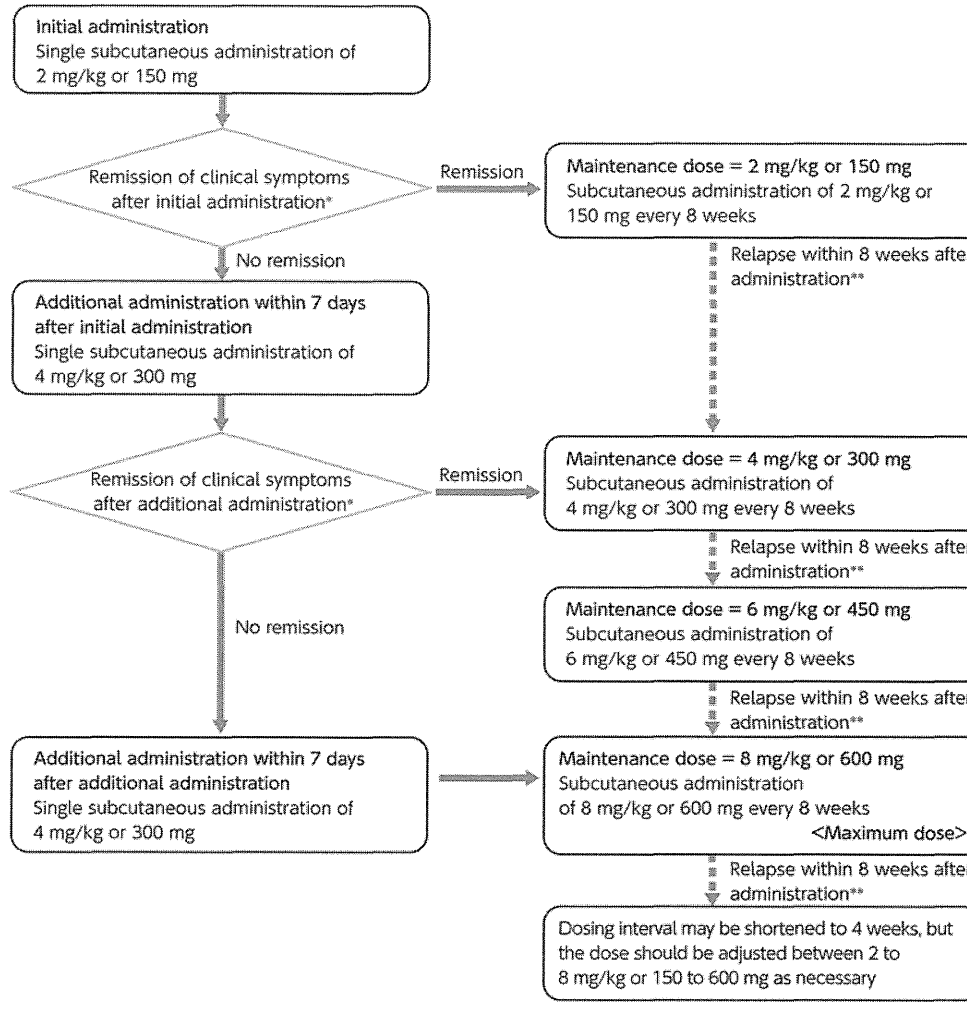

Fig. 1 Dosing regimen of canakinumab (Ilaris®) for CAPS patients [10]. Dosing regimen for CAPS patients who do not experience sufficient symptomatic relief. If sufficient clinical effects are not observed with the initial dose, the dose should be increased as shown until clinical effects are observed. The dose at which effects are observed should be the maintenance dose. * Criteria for remission in Japanese clinical studies. ** Criteria for relapse in Japanese clinical studies (modified from Ilaris® Product Information, Novartis Pharma K.K.)

Table 2 Criteria for remission and relapse used in clinical studies in Japan to evaluate the therapeutic effects of canakinumab in patients with CAPS

Remission: If the following criteria are all met, the disease is considered to have remitted	Relapse: If the following criteria are both met, the disease is considered to have relapsed
Clinical remission	Clinical relapse
Overall evaluation of autoinflammatory disease activity by physicians is minimal or lower Evaluation of skin disease is minimal or lower	Overall evaluation of autoinflammatory disease activity by physicians is mild or higher, or overall evaluation of autoinflammatory disease activity by physicians is minimal and evaluation of skin disease is mild or higher
Serological remission	Serological relapse
CRP is less than 10 mg/L (=1 mg/dL) or SAA is less than 10 mg/L (=10 μg/mL)	CRP is higher than 30 mg/L (=3 mg/dL) or SAA is higher than 30 mg/L (=30 μg/mL)

Evaluation grades are in 5 levels: absent, minimal, mild, moderate, and severe. These five levels of evaluations should be evaluated based on physician's assessment because there are no criteria for each level

education, in cooperation with physicians who have experience in the treatment of CAPS. It is the responsibility of pediatricians to optimize the effects of pharmaceutical products and minimize adverse drug reactions.

Acknowledgments The Japanese version of this work was published as a similar report in the Journal of the Japanese Pediatric Society.

Conflict of interest None.

References

1. Dinarello CA. Mutations in cryopyrin: bypassing roadblocks in the caspase 1 inflammasome for interleukin-1beta secretion and disease activity. Arthritis Rheum. 2007;56:2817–22.
2. Gattorno M, Tassi S, Carta S, et al. Pattern of interleukin-1beta secretion in response to lipopolysaccharide and ATP before and after interleukin-1 blockade in patients with CIAS1 mutations. Arthritis Rheum. 2007;56:3138–48.
3. Aganna E, Martinon F, Hawkins PN, et al. Association of mutations in the NALP3/CIAS1/PYPAF1 gene with a broad phenotype including recurrent fever, cold sensitivity, sensorineural deafness, and AA amyloidosis. Arthritis Rheum. 2002;46: 2445–52.
4. Dodé C, Le Dû N, Cuisset L, et al. New mutations of CIAS1 that are responsible for Muckle–Wells syndrome and familial cold urticaria: a novel mutation underlies both syndromes. Am J Hum Genet. 2002;70:1498–506.
5. Hoffman HM, Mueller JL, Broide DH, Wanderer AA, Kolodner RD. Mutation of a new gene encoding a putative pyrin-like protein causes familial cold autoinflammatory syndrome and Muckle–Wells syndrome. Nat Genet. 2001;29:301–5.
6. Feldmann J, Prieur AM, Quartier P, et al. Chronic infantile neurological cutaneous and articular syndrome is caused by mutations in CIAS1, a gene highly expressed in polymorphonuclear cells and chondrocytes. Am J Hum Genet. 2002;71: 198–203.
7. Church LD, McDermott MF. Canakinumab, a fully-human mAb against IL-1beta for the potential treatment of inflammatory disorders. Curr Opin Mol Ther. 2009;11:81–9.
8. Lachmann HJ, Kone-Paut I, Kuemmerle-Deschner JB, et al. Use of canakinumab in the cryopyrin-associated periodic syndrome. N Engl J Med. 2009;360:2416–25.
9. Kuemmerle-Deschner JB, Ramos E, Blank N et al.: Canakinumab (ACZ885, a fully human IgG1 anti-IL-1ß mAb) induces sustained remission in pediatric patients with cryopyrin-associated periodic syndrome (CAPS). Arthritis Res Ther. 2011;13(1):R34 (Epub ahead of print).
10. Kuemmerle-Deschner JB, Hachulla E, Cartwright R, et al. Two-year results from an open-label, multicentre, phase III study evaluating the safety and efficacy of canakinumab in patients with cryopyrin-associated periodic syndrome across different severity phenotypes. Ann Rheum Dis. 2011;70(12):2095–102.
11. Hoffman HM, Wanderer AA, Broide DH. Familial cold autoinflammatory syndrome: phenotype and genotype of an autosomal dominant periodic fever. J Allergy Clin Immunol. 2001;108: 615–20.
12. Muckle TJ, Wells M. Urticaria, deafness, and amyloidosis: a new heredo-familial syndrome. Q J Med. 1962;31:235–48.
13. Prieur AM, Griscelli C, Lampert F, Truckenbrodt H, Guggenheim MA, Lovell DJ, et al. A chronic, infantile, neurological, cutaneous and articular (CINCA) syndrome. A specific entity analysed in 30 patients. Scand J Rheumatol Suppl. 1987;66:57–68.

blood

2012 120: 1299-1308
Prepublished online June 21, 2012;
doi:10.1182/blood-2012-03-417881

Induced pluripotent stem cells from CINCA syndrome patients as a model for dissecting somatic mosaicism and drug discovery

Takayuki Tanaka, Kazutoshi Takahashi, Mayu Yamane, Shota Tomida, Saori Nakamura, Koichi Oshima, Akira Niwa, Ryuta Nishikomori, Naotomo Kambe, Hideki Hara, Masao Mitsuyama, Nobuhiro Morone, John E. Heuser, Takuya Yamamoto, Akira Watanabe, Aiko Sato-Otsubo, Seishi Ogawa, Isao Asaka, Toshio Heike, Shinya Yamanaka, Tatsutoshi Nakahata and Megumu K. Saito

Blood (print ISSN 0006-4971, online ISSN 1528-0020), is published weekly by the American Society of Hematology, 2021 L St, NW, Suite 900, Washington DC 20036.

Induced pluripotent stem cells from CINCA syndrome patients as a model for dissecting somatic mosaicism and drug discovery

Takayuki Tanaka,[1] Kazutoshi Takahashi,[1] Mayu Yamane,[1] Shota Tomida,[1] Saori Nakamura,[1] Koichi Oshima,[1] Akira Niwa,[1] Ryuta Nishikomori,[2] Naotomo Kambe,[3] Hideki Hara,[4] Masao Mitsuyama,[4] Nobuhiro Morone,[5] John E. Heuser,[5] Takuya Yamamoto,[1] Akira Watanabe,[1] Aiko Sato-Otsubo,[6] Seishi Ogawa,[6] Isao Asaka,[1] Toshio Heike,[2] Shinya Yamanaka,[1,5,7,8] Tatsutoshi Nakahata,[1,2] and Megumu K. Saito[1]

[1]Center for iPS Cell Research and Application and [2]Department of Pediatrics, Kyoto University, Kyoto, Japan; [3]Department of Dermatology, Chiba University Graduate School of Medicine, Chiba, Japan; [4]Department of Microbiology and [5]Institute for Integrated Cell-Material Sciences, Kyoto University, Kyoto, Japan; [6]Cancer Genomics Project, University of Tokyo, Tokyo, Japan; [7]Yamanaka iPS Cell Special Project, Japan Science and Technology Agency, Kawaguchi, Japan; and [8]Gladstone Institute of Cardiovascular Disease, San Francisco, CA

Chronic infantile neurologic cutaneous and articular (CINCA) syndrome is an IL-1–driven autoinflammatory disorder caused mainly by *NLRP3* mutations. The pathogenesis of CINCA syndrome patients who carry *NLRP3* mutations as somatic mosaicism has not been precisely described because of the difficulty in separating individual cells based on the presence or absence of the mutation. Here we report the generation of *NLRP3*-mutant and nonmutant-induced pluripotent stem cell (iPSC) lines from 2 CINCA syndrome patients with somatic mosaicism, and describe their differentiation into macrophages (iPS-MPs). We found that mutant cells are predominantly responsible for the pathogenesis in these mosaic patients because only mutant iPS-MPs showed the disease relevant phenotype of abnormal IL-1β secretion. We also confirmed that the existing anti-inflammatory compounds inhibited the abnormal IL-1β secretion, indicating that mutant iPS-MPs are applicable for drug screening for CINCA syndrome and other NLRP3-related inflammatory conditions. Our results illustrate that patient-derived iPSCs are useful for dissecting somatic mosaicism and that *NLRP3*-mutant iPSCs can provide a valuable platform for drug discovery for multiple NLRP3-related disorders. (*Blood*. 2012;120(6):1299-1308)

Introduction

Chronic infantile neurologic cutaneous and articular syndrome (CINCA syndrome; MIM #607715) is a dominantly inherited autoinflammatory disease characterized by systemic inflammation with an urticaria-like rash, neurologic manifestations, and arthropathy.[1] *NLRP3* mutation is the first and so far the only identified mutation that is responsible for CINCA syndrome.[2,3] *NLRP3* is expressed mainly in myelomonocytic lineage cells and chondrocytes[3] and acts as an intracellular sensor of danger signals from various cellular insults. In normal macrophages, a first stimulus, such as lipopolysaccharide (LPS), induces the synthesis of NLRP3 and the biologically inactive proIL-1β.[4] A second stimulus, such as ATP, enhances the assembly of a protein complex called the NLRP3-inflammasome.[5] The inflammasome contains caspase1, which executes the proteolytic maturation and secretion of IL-1β. Although normal monocytes/macrophages show no or limited IL-1β secretion in response to LPS stimulation alone, CINCA patients' cells exhibit robust IL-1β secretion because the mutant NLRP3-inflammasome is autoactivated without the need for any second stimulus.[6] It is therefore thought that the manifestations of CINCA syndrome are predominantly caused by the excessive secretion of the proinflammatory cytokine, IL-1β, and this concept is supported by the efficacy of an IL-1 receptor antagonist (IL-1Ra) for decreasing most of the symptoms.[7] However, because IL-1Ra treatment does not seem to ameliorate the characteristic arthropathy of cartilage overgrowth and joint contraction,[8] a more specific therapeutic approach that directly modulates the NLRP3-inflammasome is desired.

Although approximately half of CINCA patients carry heterozygous gain-of-function mutations of the *NLRP3* gene,[2,3] 30% to 40% of all patients have mutations in *NLRP3* in only a small number of somatic cells.[9,10] Because the population of mutant cells is relatively small (4.2%-35.8% in blood cells), it remains controversial whether the small fraction of *NLRP3*-mutated cells actually causes the strong autoinflammation observed in CINCA patients, or whether the *NLRP3* mutations found in mosaic patients are just a bystander, with all cells carrying an unknown mutation of another gene that causes the disease.[11]

Somatic mosaicism refers to the presence of more than 1 genetically distinct cell population in a single person, and has been identified in patients with various diseases.[12,13] The relevance of somatic mosaicism to the onset of diseases has been suggested mainly through sequence-based approaches. However, direct evidence that a cell population with a distinct genetic property shows disease-specific characteristics is lacking because it has been impossible to separately extract individual live cells from affected tissues to assess their biologic characteristics. Regarding hematopoietic disorders in which mutant cells show decreased expression of a certain protein, genetic heterogeneity caused by somatic mutations was detected by flow cytometry after intracellular staining,[14-16] but sorting out alive mutant and nonmutant cells for evaluating biologic property has been impossible.

Submitted March 27, 2012; accepted May 29, 2012. Prepublished online as *Blood* First Edition paper, June 21, 2012; DOI 10.1182/blood-2012-03-417881.

The online version of this article contains a data supplement.

The publication costs of this article were defrayed in part by page charge payment. Therefore, and solely to indicate this fact, this article is hereby marked "advertisement" in accordance with 18 USC section 1734.

Induced pluripotent stem cells (iPSCs) are pluripotent cell lines directly reprogrammed from somatic cells.[17] Patient-derived iPSCs can provide somatic cells, which cannot be directly obtained from patients, and this discovery has led to the development of a new field of disease modeling (reviewed by Grskovic et al[18]). In addition, iPSC technology has another interesting characteristic that each iPSC clone originates from a single cell,[19] which may make it possible to obtain genetically different iPSC clones from a person.

In this study, we established mutant and nonmutant iPSC lines from the same patients by deriving iPSCs from patients carrying a mutation of an autosomal gene as somatic mosaicism. By analyzing the disease-relevant characteristic of IL-1β secretion, we demonstrated that mutant macrophages are mainly responsible for the disease phenotype in the mosaic patients. Moreover, using a robust differentiation protocol to generate macrophages and purifying them by their surface marker expression, we showed that drug candidates inhibit the IL-1β secretion from mutant macrophages. Our data prove the usefulness of iPSC technology both for dissecting somatic mosaicism and as a platform for drug discovery of multiple NLRP3-related inflammatory diseases.

Methods

Human iPSC generation

We obtained skin biopsy specimens from 2 independent patients (patient 1, CIRA188Ai; and patient 2, CIRA086Ai). This study was approved by Ethics Committee of Kyoto University, and informed consent was obtained from both the patients and their guardians in accordance with the Declaration of Helsinki. We expanded the fibroblasts in DMEM (Nacalai Tesque) containing 10% FBS (Invitrogen) and 0.5% penicillin and streptomycin (Invitrogen). Generation of iPS cells was performed as described previously.[17] In brief, we introduced *OCT3/4*, *SOX2*, *KLF4*, and *c-MYC* using ecotropic retroviral transduction into fibroblasts expressing the mouse *Slc7a1* gene. Six days after transduction, the cells were harvested and replated onto mitotically inactivated SNL feeder cells. The next day, we replaced the medium with Primate ES cell medium (ReproCELL) supplemented with 4 ng/mL bFGF (Wako). Three weeks after this period, individual colonies were isolated and expanded. Cell culture was performed under 37°C, with 5% CO_2 and 21% O_2 unless otherwise stated. Cells were examined using Olympus CKX41 inverted microscope equipped with Nikon Digital Sight DS-L2 camera. A UPlan FLN 4×/0.13 objective (Nikon) was used for image acquisition.

Genetic analysis

Genomic DNA from either fibroblasts or iPSCs was isolated. The PCR product of exon 3 of *NLRP3* was sequenced directly or after subcloning with a TOPO TA cloning kit (Invitrogen), using an ABI 3100 sequencer (Applied Biosystems). For pyrosequencing, the PCR product of exon 3 of *NLRP3* was analyzed by PyroMarkQ96ID (QIAGEN).

RNA isolation and quantitative PCR for *NANOG* and the transgene

Total RNA was purified with the Trizol reagent (Invitrogen) and treated with a Turbo DNA-free kit (Ambion) to remove genomic DNA contamination. A total of 1 μg of total RNA was used for a reverse transcription reaction with ReverTraAce-α (Toyobo) and the dT_{20} primer, according to the manufacturer's instructions. Quantitative PCR was performed on the 7900HT Fast Real-Time PCR System (Applied Biosystems) with SYBR Premix ExTaqII (Takara). The primer sequences are described in supplemental Table 4 (available on the *Blood* Web site; see the Supplemental Materials link at the top of the online article).

Southern blotting

Genomic DNA (5 μg) was digested with BglII and ScaI overnight. The digested DNA fragments were separated on 1% agarose gels and were transferred to a nylon membrane (GE Healthcare). The membrane was incubated with a digoxigenin (DIG)–labeled human *cMYC* DNA probe in DIG Easy Hyb buffer (Roche Diagnostics) at 42°C overnight with constant agitation. After washing, an alkaline phosphatase-conjugated anti-DIG antibody (1:10 000; Roche Diagnostics) was added to a membrane. Signals were obtained using CDP-star (Roche Diagnostics) and detected by an LAS4000 imaging system.

Teratoma formation

Approximately 2×10^6 cells were injected subcutaneously into the dorsal flank of immunocompromised NOD/scid/γc^{null} mice (Central Institute for Experimental Animals). Masses were excised 8 to 10 weeks after injection and fixed with PBS containing 4% paraformaldehyde. Paraffin-embedded tissues were sliced and stained with hematoxylin and eosin. Slides were examined using BIOREVO BZ-9000 (KEYENCE). A PlanApo 20×/0.75 objective (Nikon) and BZ-II Viewer software (KEYENCE) were used for image acquisition.

In vitro differentiation into macrophages

Undifferentiated human embryonic stem cell (ESC) and iPSC lines were cultured on mitotically inactivated SNL feeder cells with Primate ES cell medium supplemented with 4 ng/mL bFGF. During the differentiation of the cells into macrophages, cells were cultured under 37°C, with 5% CO_2 and 5% O_2. On day 0, the iPSCs were plated at a ratio of 1:15 onto a mitotically inactivated OP9 feeder layer on 100-mm cell culture plates in α-MEM (Invitrogen) containing 10% FBS and 1% Antibiotic-Antimycotic (Invitrogen) supplemented with 50 ng/mL VEGFα (R&D Systems). On day 5, the medium was changed. On day 10, the differentiating iPSCs were collected by trypsinization, and Tra-1-85$^+$ CD34$^+$ and KDR$^+$ hematopoietic progenitors were sorted on a FACSAria II instrument (BD Biosciences). The progenitors were plated at 2×10^4 cells on another mitotically inactivated OP9 feeder layer on 100-mm cell culture plates or at 3×10^3 cells/well in 6-well cell culture plates in α-MEM containing 10% FBS and 1% Antibiotic-Antimycotic supplemented with 50 ng/mL IL-3, 50 ng/mL stem cell factor, 10 ng/mL thrombopoietin, 50 ng/mL Flt-3 ligand, and 50 ng/mL M-CSF (all R&D Systems). On day 18, the medium was changed. On day 26, differentiating cells were collected with Accumax (Innovative Cell Technologies), and CD14$^+$ iPSC-derived macrophages were purified on an autoMACSpro instrument (Miltenyi Biotec).

Peripheral blood mononuclear cells (PBs) were obtained from healthy volunteers, and CD14$^+$ monocytes were purified on the autoMACSpro instrument. For macrophage differentiation, 5×10^5 monocytes were plated in 6-well cell culture plates in RPMI 1640 (Sigma-Aldrich) containing 10% FBS and 1% Antibiotic-Antimycotic supplemented with 50 ng/mL M-CSF. On day 5, the adherent cells were collected with Accumax, and CD14$^+$ blood-derived macrophages (B-MPs) were purified on the autoMACSpro instrument. May-Giemsa–stained slides were examined using BIOREVO BZ-9000. A PlanApo 40×/0.95 objective (Nikon) and BZ-II Viewer software were used for image acquisition.

FACS analysis

Hematopoietic marker expression was evaluated on a MACSQuant Analyzer (Miltenyi Biotec). Primary antibodies Tra-1-85-FITC (R&D Systems), CD34-PE (Beckman Coulter), KDR–AlexaFluor-647 (BioLegend), CD45-PE (BD Biosciences PharMingen), and CD14-APC (Beckman Coulter) were used.

Immunocytochemistry

For immunocytochemistry, cells were fixed with PBS containing 4% paraformaldehyde for 5 minutes, permeabilized in PBS containing 0.1% Tween 20 for 5 minutes, and blocked in PBS containing 3% BSA for 10 minutes, all at room temperature. The primary antibody was for CD68 (1:50; Santa Cruz Biotechnology), and the secondary antibody was Cy3-conjugated

AffiniPure Donkey Anti–Mouse IgG (1:100; Jackson ImmunoResearch Laboratories). Nuclei were stained with 1 μg/mL Hoechst 33342 (Invitrogen). Cells were examined using BIOREVO BZ-9000. A Plan Fluor DL 10×/0.30 Ph1 objective (Nikon) and BZ-II Viewer software were used for image acquisition.

Electron microscopy

The 5×10^4 macrophages in 20 μL suspension were placed on the poly-L-lysine treated, carbon-coated sapphire disks (3 mm in diameter) and incubated for 30 minutes at 37°C with 5% CO_2. The cell-adsorbed disk was then subjected to chemical fixation with 2.5% glutaraldehyde in NaHCa buffer (100mM NaCl, 30mM HEPES, 2mM $CaCl_2$, adjusted at pH 7.4 with NaOH). These specimens were postfixed with 1% osmium and 1.5% $K_4Fe(CN)_6$ in 0.1M PBS buffer, washed, dehydrated with a series of ethanol, and embedded in Epoxy resin (TAAB EPON812). After the polymerization at 70°C, the ultra-sections (70 nm) obtained by Ultramicrotome (Leica FC6) were mounted in EM grids, stained with uranyl acetate/lead citrate, and then observed by conventional TEM (JEOL JEM1400).

PCR and microarray analysis of macrophages

Total RNA was column-purified with the RNeasy kit (QIAGEN) and treated with RNase-free DNase (QIAGEN). A total of 20 ng of total RNA was reverse transcribed into cDNA using random primers and the Sensiscript RT Kit (QIAGEN). Quantitative PCR was performed on a StepOne Plus Real-Time PCR System (Applied Biosystems) with TaqMan Gene Expression Master Mix (Applied Biosystems). The primer sequences are described in supplemental Table 4. For the microarray analysis, RNA probes were hybridized to SurePrint G3 Human GE 8 × 60K Microarrays (Agilent Technologies) according to the manufacturer's protocols. Microarrays were scanned, and the data were analyzed using the GeneSpring GX Version 11 software program (Agilent Technologies). The complete dataset from this analysis is available at the NCBI Gene Expression Omnibus using accession no. GSE38626.

LM infection

Listeria monocytogenes EGD (LM) were grown in brain heart infusion broth (Eieken Chemical), washed, suspended in PBS supplemented with 10% glycerol, and stored in aliquots at −80°C. Macrophages were seeded into an 8-well chamber slide at 2×10^5 cells/well in RPMI containing 10% FBS and then infected with bacteria at a multiplicity of infection of 10 for 60 minutes at 37°C. Cells were cultured for further 1 or 5 hours in the presence of 5 μg/mL gentamicin. The cells were fixed in 4% paraformaldehyde and incubated with PBS containing 10% Blocking One (Nacalai Tesque) and 0.1% saponin. F-actin and nuclei were visualized by staining with Alexa-488-phalloidin (Invitrogen) and 4′,6-diamidino-2-phenylindole (Dojindo), respectively. The bacteria were stained by treatment with a goat anti-*Listeria* polyclonal antibody (Kirkegaard & Perry Laboratories) and then with the Alexa 546 anti–goat IgG antibody (Invitrogen). Slides were examined using BIOREVO BZ-9000. A PlanApo_VC 100×H/1.40 objective (Nikon) and BZ-II Viewer software were used for image acquisition, and BZ-II Analyzer (KEYENCE) was used for image processing. Immunofluorescence was evaluated with the IN Cell Analyzer 2000, and samples were analyzed with the IN Cell Developer Toolbox Version 1.8 software program (GE Healthcare).

Cytokine secretion from macrophages

Purified iPS-MPs or B-MPs were seeded at the indicated counts per well or 5×10^4 cells/well unless otherwise stated in 96-well cell culture plates in RPMI 1640 containing 10% FBS and 1% Antibiotic-Antimycotic. Cells were cultured for 2 hours in the presence or absence of inhibitors. The plates were centrifuged at 300*g* for 10 minutes; then the medium was changed. Cells were cultured for 4 hours in the presence of LPS or recombinant human IL-1β. LPS concentration was 1 μg/mL unless otherwise stated. After the 30 minute or 1-hour culture after the addition of 1mM ATP (Sigma-Aldrich), we collected the supernatants and cell lysates. As second signal stimulants, we also used 500 μg/mL silica crystals (U.S. silica) for 1 hour, or 100 μg/mL monosodium urate crystals (Sigma-Aldrich) for 3 hours. For the supernatant transfer experiments, we harvested the supernatant from the wells of mutant or wild-type iPS-MPs, which were stimulated with LPS for 4 hours. After centrifugation, we transferred the supernatants to the wells of other iPS-MPs and cultured them for another 4 hours. The cytokine concentration of the supernatants was determined using a Th1/Th2 11plex FlowCytomix Kit (Bender MedSystems) following the manufacturer's instructions. Reagents were purchased as follows: CA074Me (Calbiochem), IL-1Ra (R&D Systems), oxidized ATP (oATP; Sigma-Aldrich), pyridoxalphosphate-6-azophenyl-2′,4′-disulphonic acid (PPADS; Sigma-Aldrich), cycloheximide (Sigma-Aldrich), MG132 (Calbiochem), Bay11-7082 (Sigma-Aldrich), and Ac-YVAD-CHO (Calbiochem).

LDH secretion assay

The lactate dehydrogenase (LDH) concentration of the supernatants of iPS-MPs after a 4-hour culture with LPS was determined with an LDH Cytotoxicity Detection kit (Takara) following the manufacturer's instructions.

Statistical analysis

The data were processed using the SPSS Statistics Version 18 software package. The values are reported as the mean ± SEM. Comparisons between groups were performed using the unpaired Student *t* test. $P < .05$ was considered statistically significant.

Results

Establishment and characterization of iPSCs

Dermal fibroblasts were obtained from 2 male CINCA patients who had mutations of *NLRP3* as somatic mosaicism. Both patients had nonsynonymous point mutations in the *NLRP3* coding region. The fibroblasts from patients 1 and 2 contained 34% and 9.8% mutant cells, respectively (Figure 1A; supplemental Figure 1A). These fibroblasts were reprogrammed to iPSCs after transduction with retroviral vectors encoding *OCT3/4*, *SOX2*, *KLF4*, and cMYC.[17] Twelve of the 28 isolated clones from patient 1, and 3 of 30 clones from patient 2 had a heterozygous mutation of the *NLRP3* gene, whereas the rest of the clones were wild-type (Figure 1A; supplemental Figure 1B-C). The frequency of mutants was comparable among blood cells,[9,20] fibroblasts, and iPSCs (Table 1). We randomly selected 3 mutant (M1-M3) and 3 wild-type clones (W1-W3) from patient 1 and 3 mutant (m1-m3) and 3 wild-type clones (w1-w3) from patient 2 for the propagation and subsequent analyses.

All iPSC clones showed a characteristic human ESC-like morphology (Figure 1B), the reactivation of endogenous pluripotency genes (*OCT3/4*, *SOX2*, *NANOG*; Figure 1C-D; supplemental Figure 1D) and the demethylation of the *OCT3/4* promoter regions (supplemental Figure 1E). Transgene expression was rarely detected (Figure 1D; supplemental Figure 1D), and the retroviral integration patterns were confirmed by a Southern blot analysis (Figure 1E; supplemental Figure 1F). All of the iPSC clones maintained a normal karyotype (data not shown). There were neither proviral integration nor copy number changes observed in any of the genes that might affect the function of the NLRP3 inflammasome (supplemental Tables 1 and 2). Genetic identity was proven by a short tandem repeat analysis (supplemental Table 3), and the pluripotency of the iPSC clones was confirmed by the presence of cell derivatives of all 3 germ layers by teratoma formation after injection of undifferentiated iPSCs into immunocompromised NOD/scid/γc^{null} mice (Figure 1F; supplemental Figure 1G).

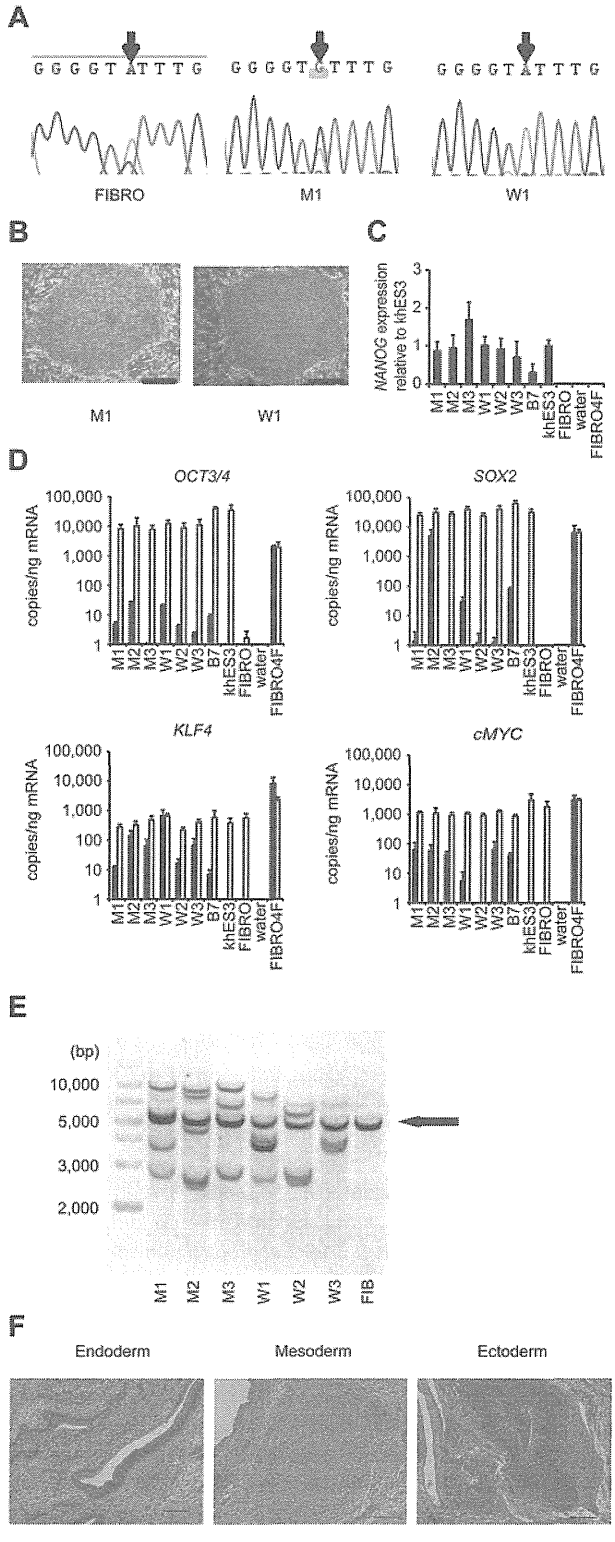

Figure 1. Establishment and characterization of iPSCs. (A) Sequencing of the *NLRP3* 1709 A > G mutation (Y570C) in fibroblasts (FIBRO), mutant iPSCs (M1), and wild-type iPSCs (W1) in patient 1. (B) The morphology of the mutant and wild-type iPSCs. (C) *NANOG* expression in CINCA iPSCs, control iPSCs (B7), control ESCs (khES3), fibroblasts (FIBRO), and fibroblasts transduced with 4 factors (FIBRO4F) normalized to *GAPDH*. n = 3. (D) A quantitative RT-PCR assay for the expression of *OCT3/4*, *SOX2*, *KLF4*, and *cMYC* in iPSCs. One primer set detects only the transgene (in black), and the other primer set detects both the transgene and endogenous gene (in white). n = 3. (E) Retroviral transgene integration analyses. Southern blot analyses were performed with DIG-labeled DNA probes against *c-MYC*. The parental fibroblasts carried a band in common with all of the iPSC lines (arrow). (F) A teratoma derived from a mutant iPSC clone, M1. Scale bars represent 100 μm. Data are mean ± SEM.

Differentiation and characterization of iPSC-derived macrophages

To compare the most prominent features of the disease, we differentiated the patient-derived iPSCs into the monocyte/macrophage lineage using a murine stromal cell line, OP9.[21] After culturing the iPSCs on an OP9 feeder layer for 10 days, we collected KDR^+ $CD34^+$ hemangioblasts (Figure 2A). All of the iPSC clones, whether they carried an *NLRP3* mutation or not, differentiated into KDR^+ $CD34^+$ progenitors as efficiently as the control ESC or iPSC clones (Figure 2B; supplemental Figure 2A). Adherent $CD68^+$ macrophages emerged after culturing the KDR^+ $CD34^+$ cells on another OP9 feeder layer for 16 days (Figure 2C; supplemental Figure 2B). Approximately 80% of the differentiated cells expressed CD14, and magnetic-activated cell sorting increased the purity to almost 100% (Figure 2D). All of the clones we used efficiently produced comparable amounts of iPSC-derived macrophages (iPS-MPs; Figure 2E; supplemental Figure 2C). The iPS-MPs visualized by light and electron microscopy showed a typical morphology, with a high cytoplasm-to-nucleus ratio and cytoplasmic vacuoles (Figure 2F; supplemental Figure 2D). The iPS-MPs showed a global gene expression pattern closer to that of blood-derived macrophages than to the parental iPSC clone (supplemental Figure 2E-F). Both mutant and wild-type iPS-MPs phagocytosed bacteria to the same extent when we infected the cells with Gram-positive LM, an intracellular bacterium that escapes into the cytosol (Figure 2G-H). These data indicate that both the mutant and wild-type iPS-MPs derived from mosaic CINCA patients are indistinguishable based on their gene expression and their phagocytic function.

Elucidation of the pathogenesis of somatic mosaic CINCA syndrome

Monocytes derived from CINCA syndrome patients usually do not spontaneously secrete IL-1β and become active after LPS stimulation.[6] Monocytes or mononuclear cells from untreated CINCA syndrome patients, however, sometimes show an increased synthesis of proIL-1β[2] and secretion of mature IL-1β,[7] even in the absence of LPS stimulation, because they can be activated by persistent inflammation or by the purification procedure. As spontaneous activation complicates the functional analysis, we herein evaluated the IL-1β activation status both before and after the stimulation. We observed that the mRNA expression of *IL1B* was low in unstimulated iPS-MPs and increased to comparable levels in mutant and wild-type iPS-MPs in response to LPS stimulation (supplemental Figure 3A). Similarly, the mRNA level of *NLRP3* was relatively low before LPS stimulation (supplemental Figure 3A). Mature IL-1β was not detectable in the supernatant of the cell culture medium (data not shown). Collectively, these data indicate that the unstimulated iPS-MPs were in an "inactive" state before stimulation.

To identify which iPS-MP clones showed the specific features compatible to patients' monocytes, we evaluated their IL-1β secretion. Although LPS stimulation alone led to IL-1β secretion

Table 1. Mutation frequency among different cell types

Patient no.	Site of mutation	Frequency (%) of mutant cells: Whole blood*	Fibroblasts	iPSCs
1	1709A > G(Y570C)	33.3	34.3	42.9
2	919G > A(G307S)	8.5	9.8	10.0

*The frequency in whole blood was reported previously.[9,20]

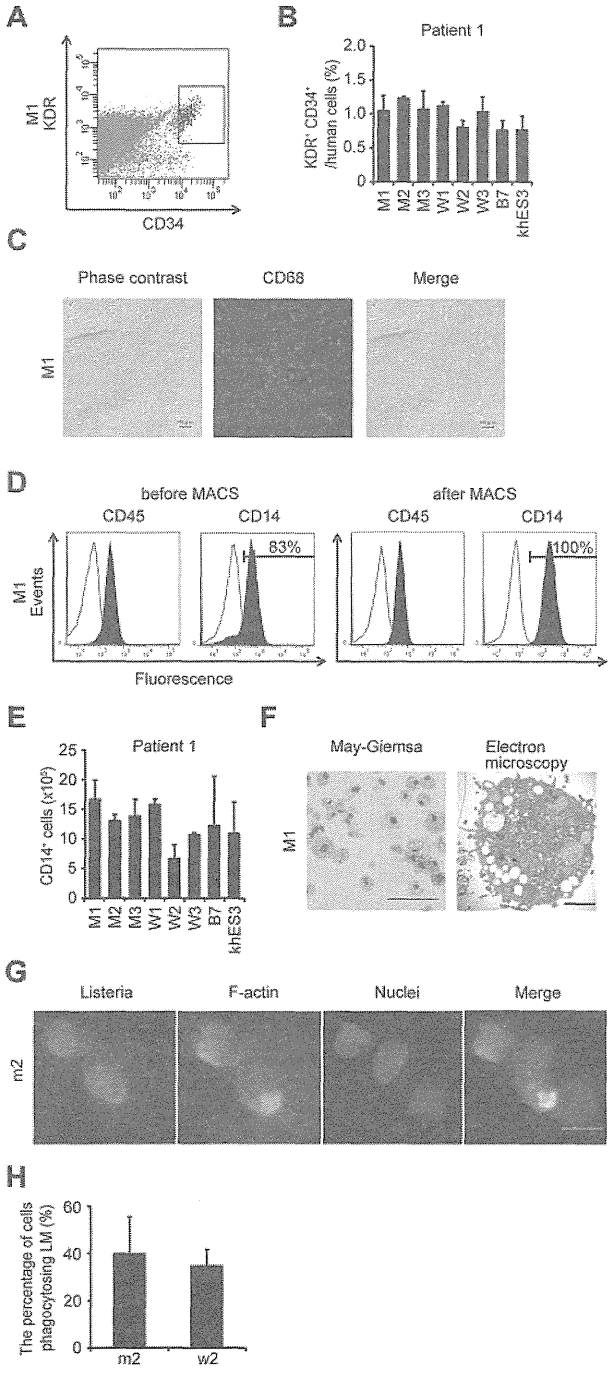

Figure 2. Differentiation and characterization of iPSCs-derived macrophages. (A) KDR^+ $CD34^+$ hematopoietic progenitors purified 10 days after differentiation. (B) The percentage of KDR^+ $CD34^+$ cells in Tra-1-85^+ human cells. n = 3. (C) CD68 immunostaining of macrophages. Scale bars represent 100 μm. (D) The histograms show antibody staining (in black) relative to the isotype-matched controls (in white) for a blood cell marker (CD45), and a macrophage marker (CD14), in cells before (left 2 panels) or after (right 2 panels) magnetic-activated cell sorting purification. (E) $CD14^+$ cell counts obtained from iPSCs plated on an OP9 feeder layer on one 100-mm dish. n = 3. (F) Representative morphology of iPS-MPs evaluated by May-Giemsa staining or transmission electron microscopy. Scale bars represent 100 μm and 2 μm, respectively. (G) The phagocytosis by iPS-MPs after LM infection. The cells were treated with anti-LM antibody, phalloidin, and 4′,6-diamidino-2-phenylindole. Scale bar represents 20 μm. (H) The percentage of iPS-MPs phagocytosing LM was calculated as the average of 9 fields of vision. Data are mean ± SEM.

from the mutant iPS-MPs, the addition of ATP was necessary to induce IL-1β secretion from wild-type iPS-MPs, as it was from either ESC-derived or blood-derived macrophages (Figure 3A). The IL-1β level from mutant iPS-MPs was significantly higher than that from wild-type macrophages, even in the presence of LPS plus ATP. Both groups of macrophages showed similar kinetics in their secretion of other cytokines, such as IL-6 or TNFα (Figure 3A). The results were similar in the iPS-MPs from patient 2 (Figure 3B). Although iPS-MPs showed a similar response at lower LPS concentrations (Figure 3C-D; supplemental Figure 3B-C), no IL-1β secretion was detectable from mutant iPSCs, wild-type iPSCs, or parental fibroblasts in response to stimulation with 1 μg/mL LPS (data not shown). These data demonstrate that the abnormal function of the iPS-MPs is predominantly determined by the *NLRP3* mutation, and not by some unknown genetic alteration(s) prevalent in all cells. We next investigated whether iPS-MPs show pyronecrosis: a pathogen-induced, cathepsin B-dependent, necrosis-like programmed cell death that is characteristically observed in *NLRP3*-mutant monocytes/macrophages.[22,23] When we compared LDH secretion as a marker of membrane rupture, we found that LPS stimulation evoked a significantly higher LDH secretion only from the mutant iPS-MPs, which was inhibited by the cathepsin B inhibitor, CA074Me (Figure 3E).

Despite the low percentage of mutant cells, the clinical manifestation of mosaic CINCA patients is similar to that of patients with a heterozygous mutation.[9,10] We hypothesized that an interaction between the mutant and wild-type macrophages leads to exacerbation of the inflammation. To test this hypothesis, we modeled a mosaic condition by coculturing mutant and wild-type cells. After stimulating mutant iPS-MPs with LPS in separate cultures or in cocultures with wild-type counterparts, we determined the IL-1β level in the supernatant. We found that the IL-1β secretion significantly increased after coculture (Figure 4A; supplemental Figure 4A). Although increasing the cell concentration raised the total amount of the IL-1β secretion from mutants, it did not accelerate the IL-1β secretion per cell from mutant iPS-MPs or enhance the secretion from wild-type macrophages (Figure 4B). To determine the ratio of mutant/wild-type cells at which the additional IL-1β secretion is most enhanced, we changed the ratio using a fixed number of mutant iPS-MPs and increasing the number of wild-type iPS-MPs. We observed a significant increase only at a percentage of 25% mutant macrophages (Figure 4C). Thus, we capitulated, at least in part, the patient's mosaic condition in vitro.

Next, we tried to elucidate whether the interaction is mediated by some humoral factor(s), but supernatant transfer did not facilitate the IL-1β secretion (Figure 4D). As a candidate that may mediate this interaction, we selected ATP because necrotic cells trigger NLRP3-inflammasome activation in part through ATP release.[24] We therefore investigated whether the necrosis-induced ATP secretion activates the wild-type iPS-MPs using ATP receptor antagonists, oxidized ATP (oATP) and PPADS. Although both antagonists markedly inhibited the IL-1β secretion after LPS plus ATP stimulation (supplemental Figure 4B), neither of them abrogated the additional IL-1β secretion in the mixed culture (Figure 4E; compare column 2 with column 3, and column 4 with column 5). The IL-1β secretion from mutant iPS-MPs may have decreased because of off-target effects of oATP.[25] Overall, although it remains to be elucidated how this effect is mediated, these results suggest that the interaction between mutant and wild-type macrophages may enhance IL-1β secretion in mosaic patients.

Validation for future applications for drug screening

An NLRP3-targeted therapeutic approach would be attractive because (1) the progressive arthropathy despite anti–IL-1 therapy indicates that the presence of additional proteins processed by the

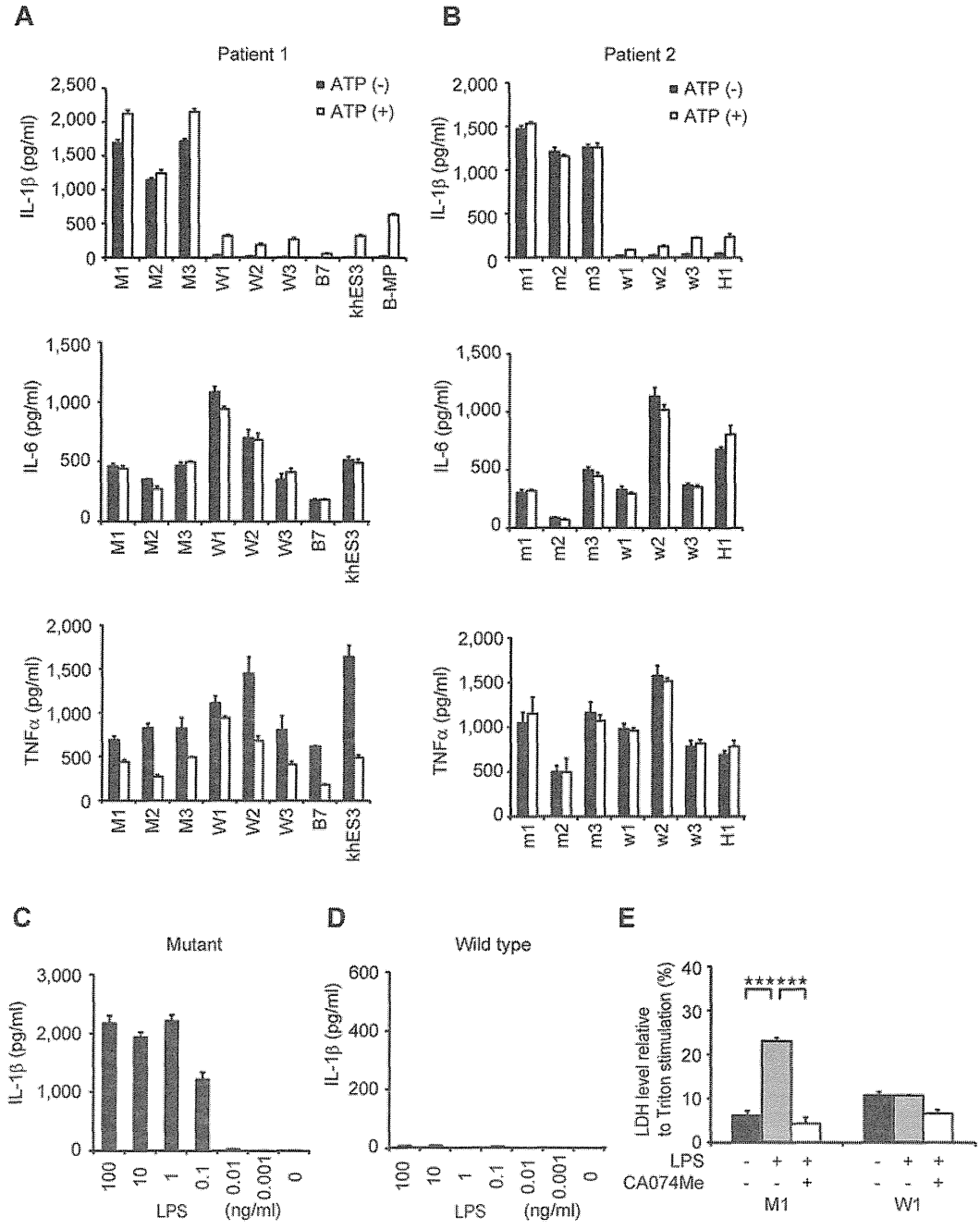

Figure 3. Elucidation of the pathogenesis of somatic mosaic CINCA syndrome. (A) Cytokine secretion from iPS-MPs derived from patient 1. After stimulating iPS-MPs by LPS with or without ATP, we determined the IL-1β (top panel), IL-6 (middle panel), or TNFα (bottom panel) level of the supernatant. n = 3. (B) Cytokine secretion from iPS-MPs derived from patient 2, determined as in panel A. (C) IL-1β secretion from mutant iPS-MPs in the presence of 10-fold dilutions of LPS from 100 ng/mL. n = 3. (D) IL-1β secretion from wild-type iPS-MPs, determined as in panel C. (E) LDH secretion from iPS-MPs stimulated with LPS in the presence or absence of the cathepsin B inhibitor, CA074Me. n = 3. Data are mean ± SEM. ***$P < .001$ (Student t test).

inflammasome is also involved in the pathogenesis of CINCA syndrome; (2) specific inhibition of the NLRP3-inflammasome can avoid unfavorable suppression of other IL-1β–processing pathways in response to various triggers; and (3) these drugs may be also effective for various other NLRP3-related chronic inflammatory conditions, such as Alzheimer disease, diabetes, severe gout, and atherosclerosis.[26-30] Because drug screening using NLRP3 autoactivated cells has not been described previously, we examined whether the iPS-MPs from CINCA patients can serve as a prototype for seeking drug candidates that directly modulate NLRP3-inflammasome activation.

When wild-type iPS-MPs were stimulated with LPS and ATP in the presence of various inhibitors, inhibitors known to modulate molecules upstream of the NLRP3-inflammasome (a protein synthesis inhibitor, cycloheximide, and an NF-κB inhibitor, MG132), downstream of the inflammasome (a caspase-1 inhibitor, Ac-YVAD-CHO), and both upstream of and the inflammasome itself[31] (Bay11-7082) successfully inhibited IL-1β secretion (Figure 5A). Although the precise mechanism is unknown, a cathepsin B inhibitor, CA074Me, also efficiently inhibited IL-1β secretion. As expected, upstream inhibitors inhibited the secretion of other cytokines, such as IL-6 and IL-8, but a downstream inhibitor,

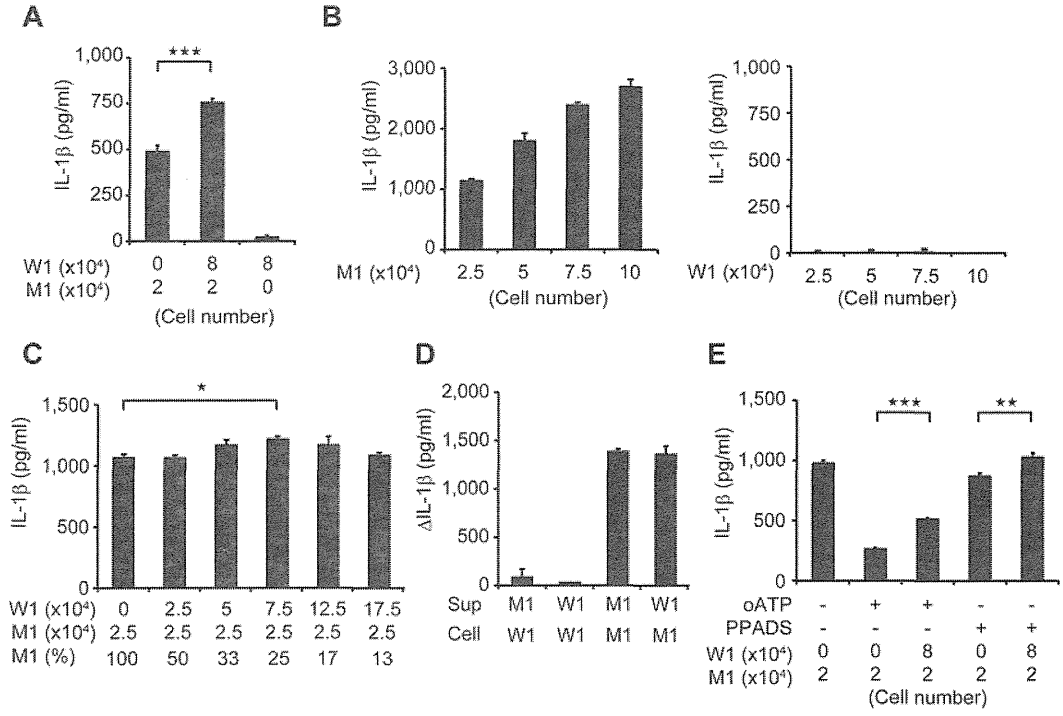

Figure 4. Remodeling mosaicism by coculturing mutant and wild-type iPS-MPs. (A) IL-1β secretion from cocultured iPS-MPs. We used 2 × 10^4 mutant iPS-MPs (M1) and 8 × 10^4 wild-type iPS-MPs (W1) as indicated. n = 6. (B) IL-1β secretion from various numbers of mutant (left panel) or wild-type (right panel) iPS-MPs. The iPS-MPs were seeded at the indicated numbers. n = 3. (C) IL-1β secretion from iPS-MPs that were cocultured at various ratios. The wild-type or mutant iPS-MPs were seeded at the numbers indicated in the first and second rows, respectively. The percentage of mutants is indicated in the third row; n = 3. (D) Increase of IL-1β levels during stimulation by the supernatant. The supernatant was harvested from the wells of the indicated iPS-MPs (Sup) and transferred to the wells of other iPS-MPs (Cell); n = 3. (E) IL-1β secretion from cocultured iPS-MPs in the presence of the ATP receptor antagonist, oATP (300μM) or PPADS (300μM). We used 2 × 10^4 mutant iPS-MPs (M1) and 8 × 10^4 wild-type iPS-MPs (W1) as indicated. n = 6. Data are mean ± SEM. ***$P < .001$ (Student t test). **$P < .01$ (Student t test). *$P < .05$ (Student t test).

Ac-YVAD-CHO, specifically affected IL-1β secretion (Figure 5A). Although CA074Me and Ac-YVAD-CHO inhibited IL-1β secretion regardless of the second signals that were present, PPADS, an inhibitor of extracellular ATP signaling, failed to inhibit IL-1β secretion by following exposure to other second signals, such as monosodium urate and silica crystals (Figure 5B), proving that wild-type iPS-MPs can be activated in a second signal-dependent manner. Therefore, the results of the wild-type iPS-MP-based compound screening depended on the choice of second signals, and such a screening makes it possible to extract candidate compounds that modulate specific second signaling pathways.

Next, we examined the response of mutant iPS-MPs to the inhibitors. In the absence of inhibitors, mutant iPS-MPs secreted a higher level of IL-1β, but treatment with inhibitors dose-dependently decreased IL-1β secretion to the comparable level produced by WT iPS-MPs (Figure 5C). We thus demonstrated the efficacy of these chemical compounds, even for excessive IL-1β production by constitutively hyperactivated inflammasomes. As expected, the mutant iPS-MPs did not respond to PPADS, confirming their autoactivation in a second signal-independent manner (Figure 5D). Therefore, because they can be activated independently from the type of second signals, mutant iPS-MP–based screening would enable the exclusion of compounds that inhibit IL-1β secretion depending on a specific type of second signal transduction. Overall, through using the IL-1β inhibition as the initial criteria and weeding out upstream inhibitors by measuring the levels of other cytokines, we can use *NLRP3*-mutant iPS-MPs to screen for drugs for CINCA syndrome and possibly for other NLRP3-related chronic inflammatory conditions.

Discussion

Since the first identification of a CINCA syndrome patient carrying *NLRP3* mutation as somatic mosaicism,[20] it has been controversial whether the small fraction of *NLRP3*-mutated cells actually causes the strong autoinflammation. It remained unanswered because of the difficulty to separately obtain live mutant and nonmutant blood cells. In this study, we reprogrammed fibroblasts from mosaic patients and obtained macrophages with different genotypes. By showing that only *NLRP3*-mutant iPS-MPs exhibit the distinct proinflammatory phenotype, we demonstrated that the *NLRP3*-mutant macrophages are mainly responsible for the pathogenesis of mosaic CINCA syndrome.

In this study, we established both *NLRP3*-mutant and nonmutant iPSC clones from the same person. One of the potential limitations of studies with patient-derived iPSCs is the difficulty in obtaining isogenic control counterparts, which do not carry the responsible mutations. One possible strategy to solve this problem is to correct the affected gene locus of patient-derived iPSC clones using novel techniques that facilitate homologous recombination.[32,33] As another solution, both affected and control iPSC clones can be obtained from patients of some X-linked hereditary diseases because each iPSC clone originated from somatic cells carrying either a mutated or nonmutated allele as an active X chromosome.[34-36] In the present study, we have retrieved both mutant and wild-type iPSC clones from patients with somatic autosomal mutations. These clones theoretically have the same genetic backgrounds, except for the *NLRP3* gene, and should serve as an ideal pair of mutant and control clones for disease research.

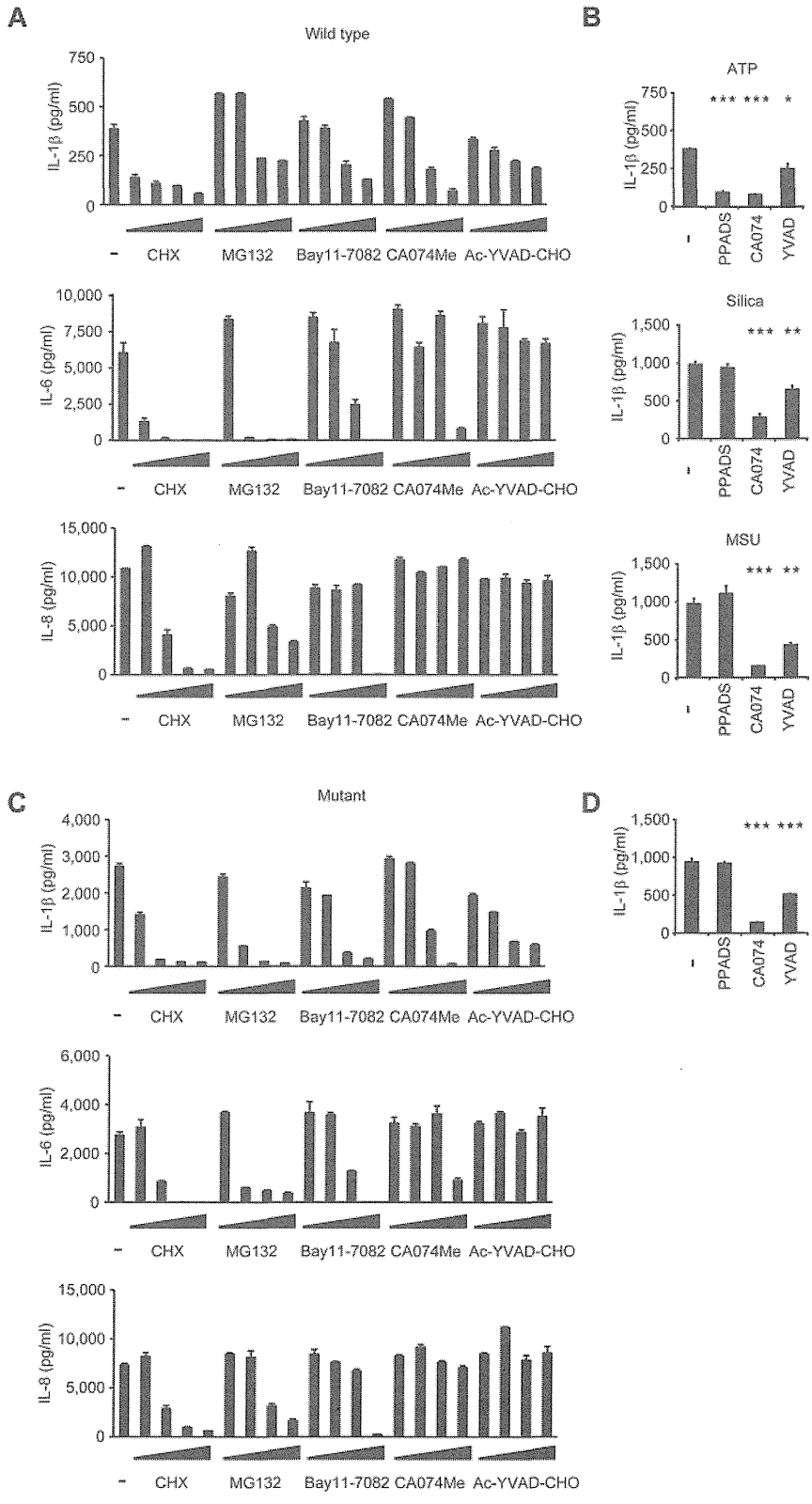

Figure 5. Validation of the cells for future applications for drug screening. (A) Inhibition of IL-1β (top panel), IL-6 (middle panel), or IL-8 (bottom panel) secretion from wild-type iPS-MPs by various inhibitors. The iPS-MPs were cultured for 2 hours in the presence of 100μM cycloheximide (CHX), 100μM MG132, 10μM Bay11-7082, 25μM CA074Me, 50μM Ac-YVAD-CHO, as well as 10-fold dilutions of each inhibitor, except CA074Me (which was diluted 5-fold), followed by LPS treatment plus ATP stimulation. n = 3. (B) The differential inhibition of IL-1β secretion from wild-type iPS-MPs by various inhibitors. In the presence of inhibitors, such as PPADS (300μM), CA074Me (25μM), or Ac-YVAD-CHO (50μM), LPS-primed wild-type iPS-MPs were stimulated with second signal triggers, such as ATP for 1 hour (top panel), silica crystals for 1 hour (middle panel), or monosodium urate crystals for 3 hours (bottom panel). n = 3. (C) Inhibition of IL-1β (top panel), IL-6 (middle panel), or IL-8 (bottom panel) secretion from mutant iPS-MPs by various inhibitors was evaluated as in panel A; n = 3. (D) Inhibition of IL-1β secretion from mutant iPS-MPs by various inhibitors. In the presence of inhibitors, such as PPADS (300μM), CA074Me (25μM), or Ac-YVAD-CHO (50μM), mutant iPS-MPs were stimulated with LPS for 4 hours. n = 3. Data are mean ± SEM. ***$P < .001$ (Student *t* test). **$P < .01$ (Student *t* test). *$P < .05$ (Student *t* test).

In addition to obtaining isogenic controls, iPSCs from patients with somatic autosomal mutations enable dissection and modeling of somatic mosaicism. Despite the fact that each person contains various minor somatic mutations,[37] the effects of mosaicism can often be overlooked because of the difficulty in assessing the possible biologic effects caused by the small cell populations carrying the genetic alterations. Here we dissected somatic mosaicism by obtaining the component cells with heterogeneous genetic identity separately and established an in vitro model to evaluate the interaction between these cells, although precise mechanism of interaction remains to be elucidated. As an approach to determining the disease-causing potential of a specific somatic mutation found in a person, iPSC technology provides advantages compared with ordinary methods, such as the use of transgenic cell lines. First,